Available online at www.sciencedirect.com
ScienceDirect
Journal of Power Sources 162 (2006) 1060–1066
JOURNAL OF POWER SOURCES
www.elsevier.com/locate/jpowsour

Growth mechanism of thin films of yttria-stabilized zirconia by chemical vapor infiltration using NiO–ceria substrate as oxygen source

Kenji Kikuchi [a,*], Koji Okada [a], Atsushi Mineshige [b]

[a] *Department of Materials Science, The University of Shiga Prefecture, 2500 Hassaka, Hikone, Shiga 522-8533, Japan*
[b] *Department of Applied Chemistry, University of Hyogo, 2167 Shosha, Himeji, Hyogo 671-2201, Japan*

Received 6 August 2006; received in revised form 24 August 2006; accepted 25 August 2006
Available online 2 October 2006

Abstract

The deposition of yttria-stabilized zirconia films on a NiO–ceria substrate by chemical vapor infiltration (CVI) using $ZrCl_4$ and YCl_3 as metal sources and NiO–ceria as oxygen source was studied. The resultant films were cubic YSZ with a Y_2O_3 content of 3.7–4.2 mol%, and were transparent and strong. A NiO content of NiO–ceria above 60 mol% increases the growth rate of the YSZ film from about 5 to 25 μm over 2 h, indicating that chemical vapor deposition (CVD) occurred in addition to electrochemical vapor deposition (EVD), whereas NiO contents below 60 mol% does not affect the growth rate, indicating that only electrochemical vapor deposition occurred. The growth mechanism of the YSZ film is determined and a YSZ thin film is successfully fabricated on NiO–ceria to improve mechanical strength.

Keywords: Yttria-stabilized zirconia; Nickel oxide; Ceria; Chemical vapor infiltration; Chemical vapor deposition; Electrochemical vapor deposition

1. Introduction

Lowering the operation temperature of fuel cells is one of the most important goals of solid oxide fuel cell (SOFC) research. Low-temperature operation of SOFCs requires a high oxide-ion conductivity and dense and thin electrolyte layers. Yttria-stabilized zirconia (YSZ) has been extensively examined as a solid electrolyte for SOFCs though its low oxide-ion conductivity requires an additional processing step at elevated temperature [1–3]. Thus, for a SOFC to exhibit higher performance at low temperatures, a thinner YSZ layer is required, while the mechanical strength of the thin film decreases with decreasing YSZ layer thickness. Electrochemical vapor deposition (EVD), as developed by Isenberg [4], is thought to be necessary for the fabrication of solid electrolyte thin films. Ogumi et al. [5] reported a modified EVD using a porous NiO as substrate and an oxygen source instead of gaseous oxygen. This technique is well-suited for the fabrication of uniform, dense, complex-shaped YSZ films formed along the surface of the NiO substrate. Ogumi et al. employed this method to fabricate a YSZ layer on a NiO pellet through a CVD–EVD process and succeeded in fabricating a YSZ microtube ca. 100 μm in diameter by the CVD–EVD process using the surface of an oxidized NiO wire as a substrate [6–9] and ceria microtubes ca. 100 μm in diameter using a NiO wire surface as oxygen source [10]. The deposition rate of the YSZ layer (1.0 μm h^{-1}) was very low. The chemical vapor infiltration (CVI) method is very effective in increasing the growth rate. CVI is widely used to fabricate composite films, for depositing carbon, silicon carbide and other materials in porous fiber preforms [11–18]. The CVI deposition rate does not depend on the specific area and substrate thickness, but rather, on the activation energy of the deposition reaction, the characteristic pore size, and properties of the gases used [19]. Furthermore, the pulsatile pressure change during CVI allows the fabrication of uniform films on a complex-shaped substrate surface. The present authors have confirmed that the modified CVI method can be employed to prepare a YSZ film on a NiO pellet at 1273–1473 K at an increased deposition rate [20]. It was found that CVD and EVD processes occurred concurrently during the growth of a YSZ layer through the CVI method; the growth rate of the YSZ film was about 5–10 times higher than the growth rate achieved by the CVD method. We succeeded in fabricating a YSZ microtube ca. 300 μm in diameter by the CVI method using the surface of an oxidized NiO wire as substrate [21]. The

* Corresponding author. Tel.: +81 749 28 8370; fax: +81 749 28 8592.
E-mail address: kikuchik@mat.usp.ac.jp (K. Kikuchi).

0378-7753/$ – see front matter © 2006 Elsevier B.V. All rights reserved.
doi:10.1016/j.jpowsour.2006.08.029

growth rate was strongly affected by the porosity of the substrate. However, the mechanical strength of the YSZ deposited was relatively low because of the delamination between the YSZ layer and NiO substrate. Moreover, it was found that controlling the composition of the YSZ film deposited by CVI was very difficult. Mineshige, a member of our research team, reported the preparation of a YSZ layer on a NiO–SDC substrate by a dissociated oxygen electrochemical vapor deposition technique [22]. He used NiO–ceria substrate as oxygen source. The growth rate of the YSZ layer was about 1.5 $\mu m\,h^{-1}$.

In the present study, CVI was employed to deposit at an increased growth rate of a dense and mechanically strong YSZ film on NiO–ceria pellets serving as oxygen source and to control the composition of the YSZ film. The present study aims to elucidate the variation in the growth mechanism of the YSZ film with NiO content of the NiO–ceria substrate.

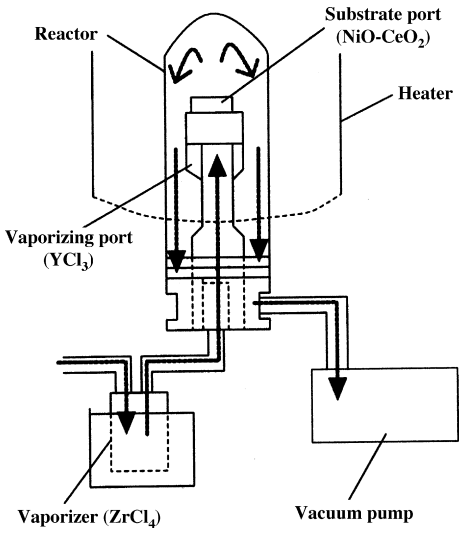

Fig. 1. A schematic of the CVI apparatus.

2. Experimental

A nickel oxide powder (99.99% purity, Kojundo Chemical Laboratory) and a ceria powder (99.9% purity, Wako) were mixed and pressed at 250 MPa to form pellets 20 mm in diameter. The pellets were sintered at 1673 K and used as substrates. Surface-oxidized Ni wires used as substrate were prepared by oxidization of nickel wire (Nilaco, 99.99% purity) in air at 1673 K for 6 h. Nickel wire diameters were 0.1, 0.3, 0.5 and 1.0 mm. Tetrachlorozirconium, $ZrCl_4$ (99.9% purity, 2 g, Kojundo Chemical Laboratory), and trichloroyttrium, YCl_3 (99.9% purity, 2 g, Kojundo Chemical Laboratory), were used as metal sources. The CVI apparatus consisted of a reactor, vaporizers, substrate port and heater as shown in Fig. 1 [20]. YCl_3 was placed on a vaporizing port in the reactor set at 1053 K, and $ZrCl_4$ was vaporized at 493–513 K. Metal chloride gases were carried with Ar or Ar containing 10 ppm hydrogen. A NiO–ceria substrate set on the substrate port was heated to 1273 K. The volume of the reactor chamber was about 100 cm^3. The flow rate of the carrier gas was adjusted to 100 and 400 $cm^3\,m^{-1}$ (STP) using control valves and flow meters. The argon contained 0.2 ppm oxygen and 5.3 ppm water as impurity. The pressure profile during each CVI run was as follows: First, the total pressure in the reactor was reduced to 600 Pa in 5 s by an oil rotary vacuum pump. Then, the carrier gas was introduced into the reactor through a control valve in 1 s, and the pressure in the reactor increased. The pressure was maintained constant for 6 s, and subsequently reduced to 600 Pa to start the next 12-s cycle. In the case of the CVD method, a CVI apparatus was used without applying the pressure profile. A constant flow rate of carrier gas of 100 $mL\,min^{-1}$ was used and the reactor pressure was maintained at about 100 Pa. The mass of $ZrCl_4$ and YCl_3 that evaporated during the CVI or CVD operations was determined by weighing the container set in the vaporizer before and after each reaction. X-ray diffraction (XRD) (Philips, X'pert-MPD) using Cu Kα was employed to analyze the thin films deposited on the NiO–ceria pellets. Their morphology was observed by a scanning electron microscope (SEM) (Hitachi, S-3200N) and laser microscope (Keyence, VF7510). The growth rate of YSZ films was estimated by measuring the films' thickness using the SEM and an electron probe micro analyzer (EPMA) (Horiba, EMAX-5770W).

3. Results and discussion

Fig. 2 shows the SEM images of the surface of YSZ films deposited on a ceria pellet substrate. The YSZ film grew with deposition time. The film was transparent, indicating that the YSZ crystal was presumably dense and pinhole-free. Its

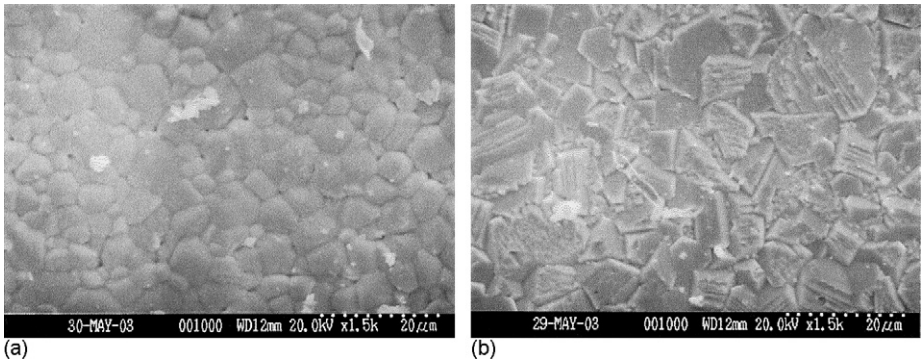

Fig. 2. SEM images of the surface of a YSZ film deposited on a ceria pellet substrate. Carrier gas: Ar. Deposition time (min): (a) 20 min and (b) 160 min.

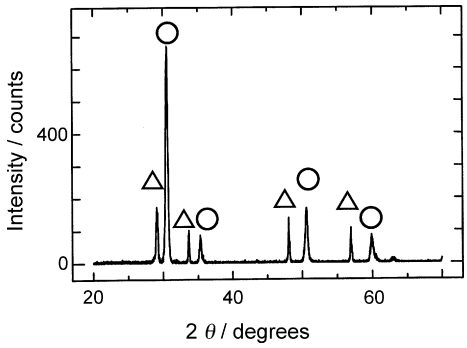

Fig. 3. XRD pattern of YSZ film deposited on a ceria pellet substrate. Carrier gas: Ar. Deposition time 80 min. ◯: YSZ, △: CeO_2.

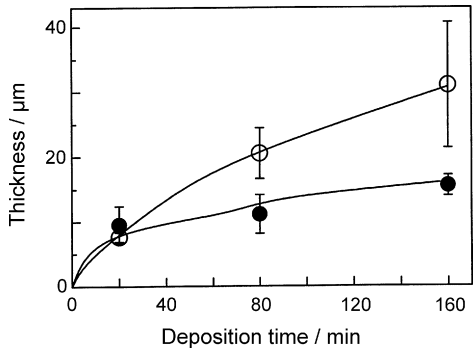

Fig. 4. Relation between deposition time and YSZ film thickness on a NiO substrate obtained by the CVI and CVD method. Carrier gas: Ar. ◯: CVI, ●: CVD.

mechanical strength was too high for peeling off by scratching with a fingernail or tweezers. When the NiO content of the NiO–ceria substrate was above 60 mol%, the resultant YSZ films were white and were too weak for use as a free-standing solid oxide electrolyte.

Fig. 3 shows the XRD pattern of a YSZ film deposited on a ceria pellet substrate in 80 min. Several peaks were assigned to YSZ and CeO. No metallic Ce peaks were observed.

Table 1 tabulates the Y_2O_3 content of a YSZ film deposited on a CeO substrate. The Y_2O_3 content showed a wide variation with the Ar carrier gas composition or a large experimental error. In the case of using Ar gas containing 10 ppm hydrogen gas, the Y_2O_3 content could be controlled precisely within an experimental error of ±0.3 mol%. The argon gas contained oxygen and water as impurities, whose reactions with metal chlorides decreased the oxygen partial pressure in the carrier gas. Thus, the partial pressures of metal chlorides, oxygen and water varied widely within a single operation cycle of 12 s. When the carrier gas contained 10 ppm hydrogen, the low partial pressure of oxygen suppressed the reaction with metal chlorides. A CVI apparatus was used for CVD, during which the flow rate of carrier gas was constant at 100 mL min^{-1}, corresponding to three times the average flow rate of carrier gas used in CVI. The Y_2O_3 content of YSZ obtained by CVD was higher than that obtained by CVI and varied widely. The zirconium chloride vapor reacted with the oxygen in the carrier gas near and in the vaporizer of zirconium chloride, resulting in a decrease in oxygen partial pressure. Since the carrier gas flowed through the zirconium chloride vaporizer to a vaporizer for yttrium chloride, the loss of yttrium chloride in the CVD method was small in comparison to that in the CVI method.

Fig. 4 shows the relation between deposition time and thickness of YSZ film on NiO substrate obtained by the CVI and CVD methods. In the case of the CVD method, the growth rate of the YSZ film within the first 20 min of deposition was almost the same as that in the case of the CVI method, and decreased after that indicating the change of the growth process from CVD to EVD using oxygen from a NiO pellet, as reported by Inaba and co-workers [7]. The mechanism of YSZ film growth during the first stage involved reactions between metal chlorides and the NiO pellet as oxygen source (CVD process):

$$ZrCl_4(g) + 2NiO(s) \rightarrow ZrO_2(s) + 2NiCl_2(g) \quad (1)$$

$$2YCl_3(g) + 3NiO(s) \rightarrow Y_2O_3(s) + 3NiCl_2(g) \quad (2)$$

Reactions between metal chlorides and oxygen gas from the dissociating NiO pellet and from the Ar carrier gas are as follows:

$$2NiO(s) \leftrightarrows 2Ni(s) + O_2(g) \quad (3)$$

$$ZrCl_4(g) + O_2(g) \rightarrow ZrO_2(s) + 2Cl_2(g) \quad (4)$$

$$2YCl_3 + \tfrac{3}{2}O_2(g) \rightarrow Y_2O_3(s) + 3Cl_2(g) \quad (5)$$

The 0.2 ppm oxygen in the argon gas was assumed to react with metal chlorides via reactions (4) and (5) and reach equilibrium concentrations within the operation time of CVI, giving an oxygen partial pressure of about 1×10^{-11} Pa for the experimental conditions used. This value is comparable to that reported in our previous paper [20]. The dissociation pressure of NiO is about 6×10^{-6} Pa at the reaction temperature [5]. Thus, the oxygen supply rate to the YSZ film was determined by reaction (3), giving a constant growth rate. A gas-impermeable YSZ layer was formed within 20 min of deposition. The EVD process of YSZ film growth proceeded as follows:

$$NiO(s) + 2e^- \rightarrow Ni(s) + O^{2-} \quad (6)$$

$$ZrCl_4(g) + 2O^{2-} \rightarrow ZrO_2(s) + 2Cl_2(g) + 4e^- \quad (7)$$

$$2YCl_3(g) + 3O^{2-} \rightarrow Y_2O_3(s) + 3Cl_2(g) + 6e^- \quad (8)$$

The YSZ growth rate should follow the parabolic law when the rate-determining step of EVD is the electrochemical transport of charged species across the YSZ film [23–25]. The parabolic law is expressed as:

$$L^2 = kt \quad (9)$$

where L denotes the YSZ film thickness, t the deposition time and k denotes the parabolic rate constant. When the oxide-ion

Table 1
Y_2O_3 content in YSZ film obtained by CVI and CVD

Method and carrier gas	Y_2O_3 content of YSZ (mol%)
CVI method (carrier gas: Ar)	1–5
CVI method (carrier gas: Ar + 10 ppm H_2)	3.7–4.2
CVD method (carrier gas: Ar)	10–15

Deposition time (min): 160.

conductivity exceeds the electronic conductivity, the parabolic rate constant k can be expressed as:

$$k = \frac{4RTV_M\sigma_e}{2nF^2}[(P_{O_2}^{II})^{-1/4} - (P_{O_2}^{I})^{-1/4}] \quad (10)$$

where σ_e is the electronic conductivity, V_M the molar volume, n the number of electrons required for producing one mole of oxide, F the Faraday constant, R the gas constant, T the deposition temperature, $P_{O_2}^{I}$ the oxygen partial pressure in the NiO–ceria pellet and $P_{O_2}^{II}$ is the oxygen partial pressure in the reactor. The oxygen partial pressure of the argon carrier gas in the reactor of the CVD apparatus was lower than that in the CVI apparatus since the argon carrier gas flowed through the zirconium chloride vaporizer at a constant rate of 100 mL min^{-1} and the operation pressure was 100 Pa in the CVD method, while in the case of CVI, the flow rate was 400 mL min^{-1} during the first second of the 12-s operation cycle and the operation pressure ranged from 100 to 600 Pa. Thus, we expected that the growth rate of the YSZ film via CVD would be larger than that via CVI. However, the growth rate of the YSZ film over 20 min of deposition was larger through CVI than through CVD since, in the case of CVI, the CVD and EVD processes occurred together using oxygen from both the carrier gas and the NiO pellet, as reported in a previous paper [20]. YSZ films deposited on the NiO substrate were white and relatively weak.

Fig. 5 shows the relation between the deposition time and thickness of YSZ film on a ceria substrate obtained by the CVI and CVD methods. YSZ films deposited on the CeO_2 substrate were transparent and strong. The growth rate of YSZ films deposited on ceria was lower than that of YSZ films deposited on nickel oxide. The thickness of the YSZ film within the first 20 min of deposition increased with the deposition time. After 20 min of deposition, the growth rate of the YSZ film suddenly decreased. Similar trends were observed in the case of the NiO pellet, even though the growth mechanism was thought to be different in the two cases since the color and mechanical strength of the film obtained on the ceria substrate differed from those of the film obtained on the NiO pellet. The thickness of the YSZ film deposited on the NiO pellet in 20 min (∼10 μm) was larger than that deposited on the ceria pellet (5 μm). During the first stage, the metal chloride reacts directly with the ceria substrate, which is indicative of the CVD process.

$$ZrCl_4(g) + 4CeO_2(s) \rightarrow ZrO_2(s) + 2Ce_2O_3(s) + 2Cl_2(g) \quad (11)$$

The decomposition of nickel oxide and the disproportionate reaction of ceria yielded oxygen as follows:

$$2CeO_2(s) \leftrightarrows Ce_2O_3(s) + \tfrac{1}{2}O_2(g) \quad (12)$$

$$K_1 = \frac{a_{Ce_2O_3}P_{O_2}^{1/2}}{a_{CeO_2}^2} \quad (13)$$

The value of K_1 at 1273 K is 1.5×10^{-6} Pa$^{1/2}$ [26], which gives a dissociation pressure of about 2.2×10^{-12} Pa. The oxygen supply rate to the growing YSZ film from ceria was thought to be lower than that from nickel oxide. Thus, at deposition times below 20 min, the high growth rate of the YSZ film on the NiO pellet yielded a thicker YSZ film compared to that grown on the ceria pellet. At a deposition time of 20 min, the thickness of the YSZ film grown by the CVD method was higher than that grown by the CVI method. This trend was exactly the reverse of that observed in Fig. 4. A low oxygen partial pressure was found to accelerate reaction (12), giving a thick YSZ film. The rate-determining factor of YSZ film growth seemed to be supply rate of oxygen ions from ceria to the YSZ film since the growth rate was almost the same within the first 10 min of deposition even though the oxygen partial pressure in the CVD apparatus was different from that in the CVI apparatus. During the next stage, the growth mechanism of the YSZ film was thought to involve the EVD process, and the reaction between the metal chlorides and oxygen ions from ceria was as follows:

$$2CeO_2(s) + 2e^- \rightarrow Ce_2O_3(s) + O^{2-} \quad (14)$$

This reaction was followed by reactions (7) and (8). At a deposition time of 80 min, the growth rate of the YSZ film by CVI and CVD was about 0.5 and 2 μm h^{-1}, respectively. The oxygen partial pressure near the substrate surface in the CVD method was lower than that in the CVI method. Thus, it was concluded that the growth of the YSZ film in this region involved the EVD process.

Fig. 6 shows the effect of the NiO content of the substrate on the growth rate of YSZ film deposited on NiO–ceria substrate.

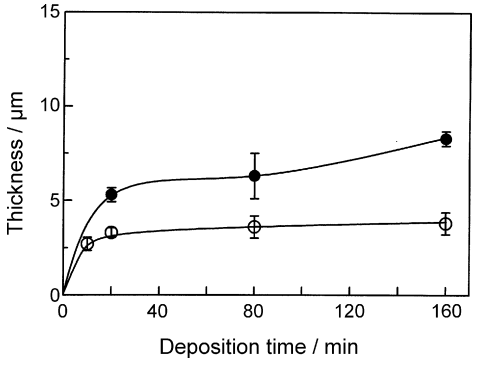

Fig. 5. Relation between deposition time and YSZ film thickness on a ceria substrate obtained by the CVI and CVD method. Carrier gas: Ar. ◯: CVI, ●: CVD. Flow rate of carrier gas (mL min^{-1}); CVI: 400; CVD: 100.

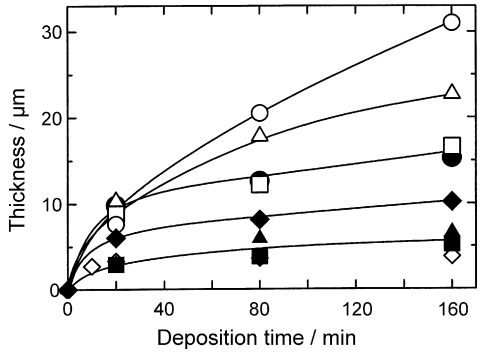

Fig. 6. Effect of NiO content of substrate on the growth rate of YSZ film. Carrier gas: Ar. NiO content (mol%); ◯: 100, △: 92.0, □: 77.6, ●: 69.7, ▲: 60.6, ■: 36.5, ◇: 0, ◆: 36.5 (Ar + 10 ppm H_2).

A decrease of NiO content from 100 to 69.7 mol% reduced the growth rate of the YSZ film. The thickness of the YSZ film remained almost constant despite a further decrease in NiO content below 60.6 mol%. Since the YSZ film thickness did not change within the first 20 min of deposition at NiO contents above 69.7 mol%, the supply rate of oxygen from the NiO substrate to the growing YSZ film seemed to remain constant, and the CVD process predominated. The deposition time versus thickness curves almost coincided at NiO contents below 60.6 mol%. This indicates that the same growth mechanism is at play. The growth rate was higher in the argon carrier gas containing 10 ppm hydrogen than in argon carrier gas. The oxygen contained in the argon carrier gas as impurity reacts with the hydrogen gas contained in the carrier gas and metal chlorides via reactions (4) and (5) and the following reactions:

$$H_2 + Cl_2 \leftrightarrow 2HCl \quad (15)$$

$$2H_2 + O_2 \leftrightarrow 2H_2O \quad (16)$$

The oxygen partial pressure in the carrier gas was estimated to be about 2.0×10^{-24} Pa under the present experimental conditions, with the assumption that the reactions attained equilibrium within the operation time of CVI. Since the growth rate of the YSZ film under Ar + 10 ppm H_2 was higher than that under Ar, it was concluded that growth occurred via the EVD process at NiO contents below 60.6 mol%.

Fig. 7 plots deposition time versus the square of YSZ film thickness. Fig. 7A shows a straight line, indicating that the growth rate of the YSZ film followed the parabolic law expressed by Eq. (9). The parabolic rate constant, k, obtained by Eq. (10) related to the difference in the oxygen partial pressure across the growing YSZ film. The value of k decreased with decreasing NiO content of NiO–ceria substrate, indicating that the decrease in the growth rate was due to the decrease in the oxygen partial pressure, $P^{I}_{O_2}$, at the interface between the substrate and YSZ film since the oxygen supply rate from the substrate to the growing YSZ film decreased. It is found that the main rate-determining step of YSZ film growth by CVI is the electrochemical transport of charged species. Fig. 7B shows the plots for the case of NiO content below 60.6 mol%. The CVD process proceeded during the first 20 min of deposition and yielded a dense film. After 20 min, the growth mechanism changed from CVD to EVD, resulting in a lower growth rate compared to the CVD process. The value of k seemed to approach 0 as the NiO content decreased to zero. The dissociation pressure of ceria at 1273 K is 2.2×10^{-12} Pa and the oxygen partial pressure of the argon carrier gas was about 1.0×10^{-11} Pa, indicating that the difference between $P^{I}_{O_2}$ and $P^{II}_{O_2}$ was very small or negative in sign. The deviation from stoichiometry of ceria was reported by Tuller and Nowick [28]. The value of x in CeO_{2-x} is 0.1 at an oxygen partial pressure of 1.0×10^{-11} Pa. However, at a NiO content of zero, the partial pressure of oxygen, $P^{I}_{O_2}$, could not be maintained during CVI operation since the diffusion rate of oxygen ions in ceria might not be sufficiently high. The oxygen partial pressure in the argon carrier gas decreased from 1.0×10^{-11} to 1.0×10^{-24} Pa with the addition of 10 ppm hydrogen gas to the carrier gas. The electric conductivity of YSZ increased with the decrease of oxygen partial pressure and the value of it at the low oxygen partial pressure of 1.0×10^{-24} Pa had to be not negligible. Then the value of σ_e, in Eq. (10) increased. Moreover, the difference of the oxygen partial pressure across the growing YSZ film increased. Thus, the value of k increased and at NiO contents below 36.5 mol%, the YSZ film grew with deposition time.

Fig. 8 shows the effect of NiO content on the gap between the substrate and YSZ film deposited on the NiO–ceria substrate by the CVI method. We reported a gap forming between the YSZ film and NiO substrate [20]. The gap decreased from 55 to 0 μm as the NiO content decreased from 100 to 60.6 mol%. The volume of the substrate decreased with decreasing NiO content. At a NiO content of 100 mol%, the decrease in volume at 298 K was estimated to be about 40.7% on the basis of the densities of NiO and metal Ni, which are 6.72 and 8.90 g cm^{-3}, respectively

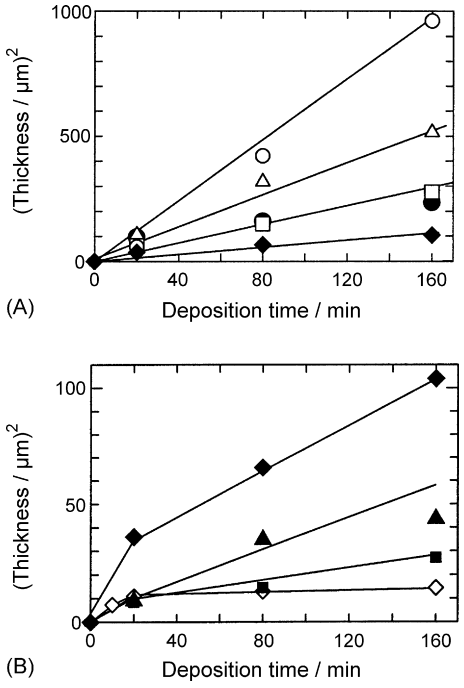

Fig. 7. Effect of NiO content of substrate on the growth rate of YSZ film. Carrier gas: Ar. NiO content (mol%); ○: 100, △: 92.0, □: 77.6, ●: 69.7, ▲: 60.6, ■: 36.5, ◇: 0, ◆: 36.5 (Ar + 10 ppm H_2).

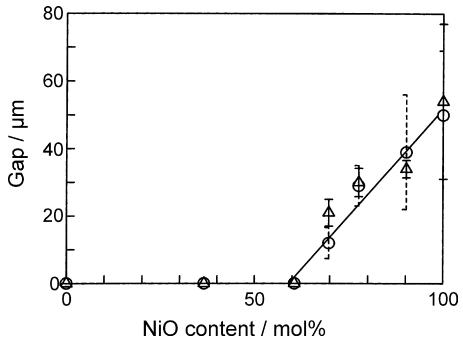

Fig. 8. Effect of NiO content on a gap between the substrate and YSZ film deposited on a CeO_2–NiO_2 substrate obtained by the CVI method. Deposition time (min): 160. Carrier gas: ○: Ar, △: Ar + 10 ppm H_2.

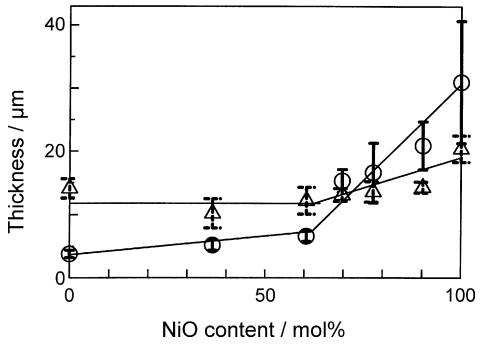

Fig. 9. Dependence of the NiO content of substrate on the thickness of YSZ film obtained by the CVI method. Deposition time (min): 160. Carrier gas: ◯: Ar, △: Ar + 10 ppm H_2.

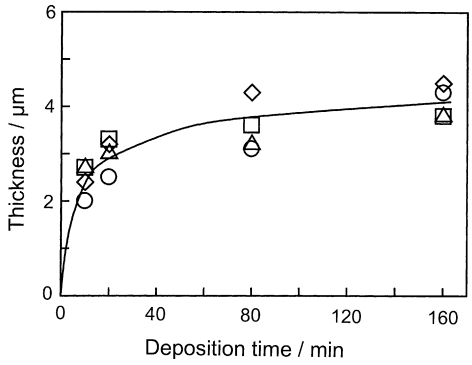

Fig. 10. Effect of the thickness of CeO_2 substrate on the growth rate of the YSZ film. Carrier gas: Ar. Thickness of CeO_2 (mm); ◯: 1.0, △: 2.0, □: 3.0, ◊: 4.0.

[27]. At a CeO_2 of 100 mol%, the densities of CeO_2 and Ce_2O_3 at 25 °C were 7.65 and 6.20 g cm^{-3}, respectively, indicating an increase of volume of about 17.6%. Thus, rate of decrease of the substrate volume decreased with decreasing NiO content of NiO–ceria substrate, and the variation of substrate volume changed from volume decrease to volume increase at a NiO content of about 43.6 mol%, which was estimated by calculation of the densities. However, the change was observed to occur at a NiO content of about 60 mol%. The density of the substrate was about ca. 73% of the theoretical value, and a frame built with CeO_2 at NiO contents below 60 mol% may be kept despite the reduction of NiO. Thus, the observed value of 60 mol% differed from the calculated value.

Fig. 9 shows the dependence of NiO content of substrate on YSZ film thickness at a deposition time of 160 min obtained by the CVI method. The YSZ film thickness at NiO contents above 60.6 mol% increased with NiO content, while, below 60.6 mol%, the thickness increased little or was almost constant with increasing NiO content. In the case of the 100 mol% NiO pellet, the growth mechanism of YSZ changed from CVD to EVD in addition to CVD by the formation of gas-impermeable YSZ film and the CVI method enhanced the CVD process using oxygen in the carrier gas, as reported in our previous paper [20]. At NiO contents above 60.6 mol%, YSZ films grown with Ar were thicker than those grown with Ar containing 10 ppm hydrogen since the oxygen partial pressure of the carrier gas decreased. At NiO contents above 70 mol%, the YSZ films were white, whereas those below 60.6 mol% were transparent. It is found that the growth process of YSZ changed dynamically at a NiO content of about 60 mol%. The gap between YSZ film and substrate was zero at NiO contents below 60.6 mol%. Thus, the presence of the gap was thought to enhance the dissociation of NiO and

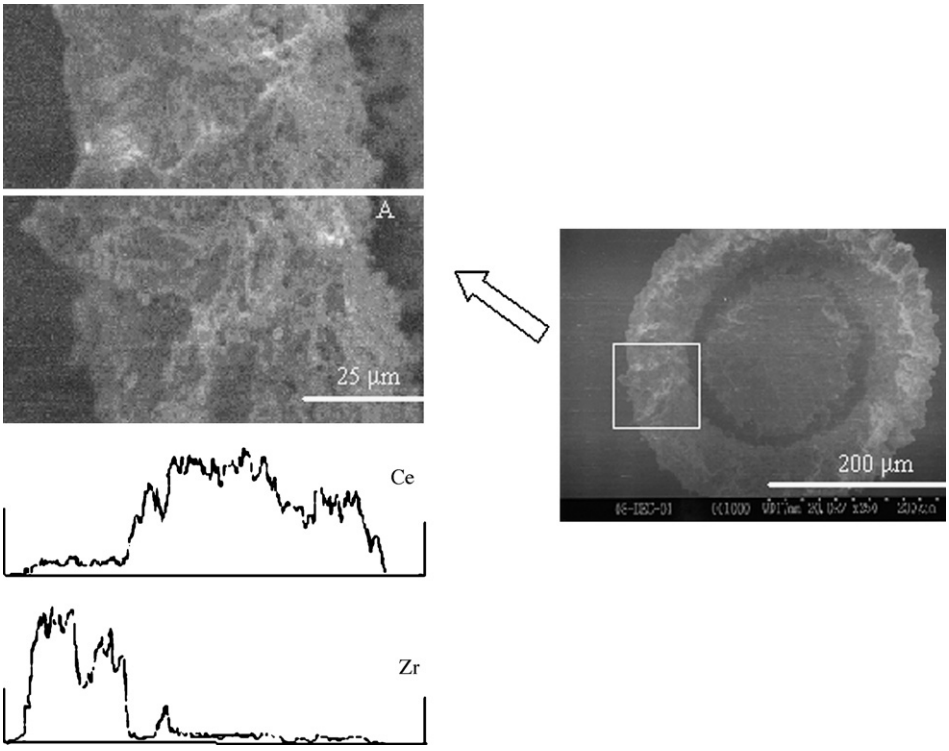

Fig. 11. SEM image and line analysis by EPMA of a YSZ film deposited on a hollow CeO_2 fiber.

promote the CVD process, its absence suppressing the dissociation of NiO and accelerating the EVD process. At NiO contents below 60.6 mol%, the YSZ film thickness decreased slightly with decreasing NiO content, indicating that $P^{I}_{O_2}$ decreased with decreasing NiO content. The YSZ film was thicker at lower oxygen partial pressures (Ar + 10 ppm H_2) than at higher oxygen pressures (Ar); its thickness was almost constant despite the change in NiO content. The value of k seemed to be constant below a NiO content of 60.6 mol% since the EVD process was dominant in YSZ film growth. In the case of argon gas containing 10 ppm hydrogen, the oxygen partial pressure of the reaction gas ($\sim 10^{-24}$ Pa) was too low to change the value of k since the second term on the right-hand side of Eq. (10) was negligible compared to the first term.

The effect of the thickness of the ceria substrate on the growth rate of the YSZ film was examined to determine the mechanism for oxygen transfer from substrate to YSZ film, as shown in Fig. 10. The YSZ film thickness was almost constant with deposition time within experimental error despite the change of ceria substrate thickness. Under the present experimental conditions, YSZ film growth occurred only through the EVD process. At an oxygen partial pressure of 1×10^{-11} and 1×10^{-24} Pa, the value of x in CeO_{2-x} is about 0.1 and 0.4, respectively, at 1273 K [28]. If the diffusion rate of oxygen in ceria were enough to compensate for the oxygen defects formed by the disproportionate reactions, the value of $P^{I}_{O_2}$ would be expected to increase with the thickness of the NiO–ceria substrate, and thicker YSZ films would be obtained using thicker ceria substrates. However, the YSZ film thickness was independent of the thickness of the ceria substrate. The value of $P^{I}_{O_2}$ did not change with the thickness of ceria, indicating that the thickness had to be larger than 0.5 mm to be able to provide oxygen to the growing YSZ film.

Fig. 11 shows SEM images and line analysis results obtained by EPMA of a YSZ film deposited on a hollow ceria fiber. The hollow CeO_2 fiber was fabricated on an oxidized Ni wire substrate with the CVD method, as detailed in the literature [9]. The line analysis results indicated that there was a ceria layer on the NiO wire and that a YSZ film was fabricated on the ceria layer. There was a gap between the NiO substrate and ceria, but no gap was observed between the ceria and YSZ film. The thickness of the ceria layer deposited on the NiO wire substrate was about 40 μm, and the thickness of the YSZ film deposited on the ceria layer was about 10 μm. It was found that the complex solid oxide film could be fabricated by the CVD and CVI methods.

4. Conclusion

A YSZ film was successfully fabricated on a NiO–ceria substrate by the CVI method at a high growth rate that ranged from 3 to 12 μm h^{-1}. The gap between the YSZ film and substrate increased from 0 to 50 μm with increasing NiO content above 60.6 mol%. The growth mechanism changed at a NiO content of 60.6 mol% presumably because the absence of a gap suppressed the dissociation of NiO. The value of $P^{I}_{O_2}$ seemed to be controlled by the NiO content of the substrate. The resulting YSZ film was transparent and had high mechanical strength, and thus showed promise as electrolyte material for SOFCs.

References

[1] J. Weissbart, R. Ruka, J. Electrochem. Soc. 109 (1962) 723.
[2] D.J.M. Burkhard, B. Hanson, G.C. Ulmer, Solid State Ionics 47 (1991) 169.
[3] H. Koide, Y. Someya, T. Yoshida, T. Maruyama, Solid State Ionics 132 (2000) 253.
[4] A.O. Isenberg, Solid State Ionics 3–4 (1981) 431.
[5] Z. Ogumi, T. Ioroi, Y. Uchimoto, Z. Takehara, T. Ogawa, K. Toyama, J. Am. Ceram. Soc. 78 (1995) 593.
[6] M. Inaba, A. Mineshige, S. Nakanishi, N. Nishimura, A. Tasaka, K. Kikuchi, Z. Ogumi, The Solid Films 323 (1998) 18.
[7] A. Mineshige, M. Inaba, Z. Ogumi, T. Takahashi, T. Kawagoe, A. Tasaka, K. Kikuchi, J. Am. Ceram. Soc. 78 (1995) 3157.
[8] A. Mineshige, M. Inaba, Z. Ogumi, T. Takahashi, T. Kawagoe, A. Tasaka, K. Kikuchi, Solid State Ionics 86–88 (1996) 251.
[9] M. Inaba, A. Mineshige, T. Maeda, S. Nakanishi, T. Takahashi, A. Tasaka, K. Kikuchi, Z. Ogumi, Solid State Ionics 93 (1997) 187.
[10] M. Inaba, A. Mineshige, T. Maeda, S. Nakanishi, T. Ioroi, T. Takahashi, A. Tasaka, K. Kikuchi, Z. Ogumi, Solid State Ionics 104 (1997) 303.
[11] P. Mcallister, E.E. Wolt, Carbon 129 (1991) 387.
[12] B.W. Sheldon, T.M. Besmann, J. Am. Ceram. Soc. 74 (1991) 3046.
[13] T. Tago, M. Kawase, K. Morita, K. Hashimoto, J. Am. Ceram. 82 (1999) 3393.
[14] R.I. Baxter, R.D. Rawlings, N. Iwashita, Y. Sawada, Carbon 38 (2000) 441.
[15] N. Yoshikawa, A. Kikuchi, S. Taniguchi, Key Eng. Mater. 161–163 (1999) 275.
[16] S. Bertrand, O. Boisron, R. Pailler, J. Lamon, R. Naslan, Key Eng. Mater. 164–165 (1999) 357.
[17] R.R. Naslain, Key Eng. Mater. 164–165 (1999) 3.
[18] T. Hirata, E. Asari, M. Kitajima, J. Solid State Chem. 110 (1994) 201.
[19] S.K. Griffiths, R.H. Nilson, in: Jong-Hee Park, T.S. Sudarshan (Eds.), Chemical Vapour Deposition, ASM International, Materials Park, 2001, pp. 183–203 (Chapter 6).
[20] K. Kikuchi, T. Okaya, W. Hirose, K. Matsuo, A. Mineshige, Z. Ogumi, J. Electrochem. Soc. 150 (2003) C688.
[21] K. Kikuchi, O. Matsuo, A. Mineshige, Z. Ogumi, Solid State Ionics, in press.
[22] A. Mineshige, K. Fukushima, K. Tsukada, M. Kobe, T. Yazawa, K. Kikuchi, M. Inaba, Z. Ogumi, Solid State Ionics 175 (2004) 483.
[23] Y.S. Lin, L.G.J. de Haart, K.J. de Vriers, A.J. Burggraaf, J. Electrochem. Soc. 137 (1991) 3960.
[24] J. Schoonman, J.P. Dekker, J.W. Broerss, Solid State Ionics 46 (1991) 299.
[25] U.B. Pal, S.C. Singhal, J. Electrochem. Soc. 137 (1990) 2937.
[26] Barin Ihasan, Thermodynamic Data of Pure Substances, VCH, Weinheim, 1993, p. 383, p. 1067.
[27] David R. Lide, CRC Handbook of Chemistry and Physics, 86th ed., CRC Press Taylor & Francis, Boca Raton, 2005, pp. 4–56.
[28] H.L. Tuller, A.S. Nowick, J. Electrochem. Soc. 126 (1979) 209.